Description of Soft Diffraction in the Framework of Reggeon Calculus. Predictions for LHC

Alexei Kaidalov[1], *Martin Poghosyan*[2]

[1] Institute of Theoretical and Experimental Physics, 117526 Moscow, Russia
[2] Università di Torino and INFN, 10125 Torino, Italy

A model, based on Gribov's Reggeon calculus, is proposed and applied to processes of soft diffraction at high energies. It is shown that by accounting for absorptive corrections for all legs of triple-Regge and loop diagrams a good description of experimental data on inelastic soft diffraction can be obtained. In this paper we give a brief description of the model and of its predictions for LHC energies.

1 Introduction

The process of soft single- and double- diffraction dissociation are closely related to small angle elastic scattering in which each of the incoming hadrons may become a system which will then decay into a number of stable final state particles. Regge-pole theory is the main method for description of high-energy soft processes. In this approach (see [1]), the inclusive cross-section of single and double diffraction dissociations is described by triple-Reggeon and loop diagrams, respectively. Triple-Reggeon description is in good agreement with the FNAL and ISR data for soft diffraction dissociation [2]. However, the higher-energy data from SPS and Tevatron do not show the increase of the cross section with energy expected from the simple fits and the contribution of triple-Pomeron vertex (in the elastic scattering amplitude) violates unitarity. A number of different approaches have been proposed in order to be in agreement with the data from higher energy experiments: non-gaussian parameterisation for Reggeon-hadron vertex [3], renormalisation [4] or damping [5] of the Pomeron flux. A more realistic approach suggested in [6] and [7] by the inclusion of initial state elastic scattering corrections to the triple-Reggeon vertices. However, the analysis done in [8] shows that this correction is not enough for restoring the s-channel unitarity.

Besides of its own role, the theoretical knowledge of soft diffraction is also important in analysing hard diffraction data, which is an active area of study at HERA and Tevatron and will continue to be interesting at LHC. The knowledge of the interaction between Pomerons (enhanced diagrams) is important for analysing data at very high energies, too. The contribution of these diagrams can be essential in hadron-nucleus and especially in nucleus-nucleus collisions, where the thermalisation and the quark-gluon plasma formation strongly depend on the strength of interactions between Pomerons [9].

In this article we propose to describe data on soft diffraction dissociation in pp and $p\bar{p}$ interactions taking into account all possible non-enhanced absorptive corrections to triple-Regge vertices and loop diagrams. This approach describes available data on high-mass soft diffraction in the energy range from ISR, FNAL to Tevatron. The article is organised as follows: In the next

two sections we briefly describe the Regge-pole approach, Gribovs' Reggeon calculus and AGK cutting rules. Our proposed model is presented in Section 4 and its predictions are compared with data in Section 5.

2 Single Regge-Pole Approximation

In Regge theory, the simplest singularity in the j-plane is a moving pole $\alpha(t)$ in the t-channel (see the leftmost graph in Fig. 1) and in the small t-region the scattering amplitude, $M(s,t)$, of the process $a+b \to c+d$ can be parameterised as:

$$M(s,t) = \gamma(0)\eta(\alpha(0))(s/s_0)^{\alpha(0)-1} \exp(\lambda(s)t). \tag{1}$$

Here $\eta(\alpha(t))$ is the signature factor, $\gamma(t) \equiv g_{ac}(t)g_{bd}(t)$ is the factorisation residue, and $\lambda(s) = R^2 + \alpha'_R \ \ln(s/s_0)$. The parameter R^2 characterises the t-dependence of the product of residue function and of the signature factor. In our notations the normalisation of the scattering amplitude is such that $\sigma_{tot} = 8\pi \,\mathrm{Im}\, M(s,0)$ and $d\sigma_{el}/dt = 4\pi|M(s,t)|^2$.
Because the Pomeron's intercept is larger than unity (which is required in order to guarantee the growth of the total cross-section, $\sigma_{tot} \sim s^{\Delta}$ where $\Delta \equiv \alpha_P(0) - 1$), the corresponding cross-section grows as a power function of s and therefore the contribution of the Pomeron-pole in the scattering amplitude violates unitarity. The easiest way to restore the unitarity is to take into account branch points which correspond to multi-Reggeon exchange. The calculation of the multi-Reggeon exchange amplitude is possible in eikonal (or eikonal-like) approximation, where only single particle intermediate states are taken into account.

3 Eikonal Approximation and AGK Cutting Rules

Regge poles are not the only singularities in the complex angular momentum plane. Exchange of several Reggeons in t-channel leads to moving branch points in the j-plane (Fig. 1). A Regge pole exchange can be interpreted as corresponding to single scattering while Regge cuts correspond to multiple scatterings on constituents of hadrons. In case of the 'supercritical' Pomeron ($\Delta > 0$) the contribution of n-Pomeron exchange in the scattering amplitude ($M_P^{(n)}(s,0) \sim s^{n\Delta}$) is increasing with the increase of the energy and the entire series of n-Pomeron exchange should be summed. On the contrary, the contribution of the branch points

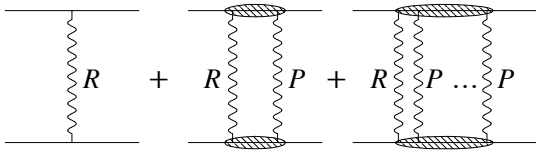

Figure 1: Single pole and RP^n cut contribution in the elastic scattering amplitude. R stands for secondary Reggeon and for Pomeron.

concerned with the exchange of several secondary Reggeons decreases very quickly with increasing collision energy and the contribution of such branch points can be neglected with respect to the branch points due to the exchange of one secondary Reggeon and Pomerons that are needed for properly matching low energy data. For instance, in eikonal approximation the amplitude

of n-Pomeron exchange can be written in the following form [10]:

$$M^{(n)}(s,t) = \frac{(2i)^{n-1}}{n!} \int \prod_{i=1}^{n} \left[M^{(1)}(s, \mathbf{q}_{i\perp}^2) \frac{d^2\mathbf{q}_{i\perp}}{2\pi} \right] \delta \left(\mathbf{q}_\perp - \sum_{i=1}^{n} \mathbf{q}_{i\perp} \right). \qquad (2)$$

Using the parameterisation (1) for the Regge pole contribution and performing the integration over the transverse momenta of Reggeons in Eq. (2) it can be shown that the account of the multi-Pomeron exchanges results in the unitarisation of the scattering amplitude, which leads to the Froissart behaviour of the total cross section for $s \gg m_N^2$: $\sigma_{tot} \simeq 8\pi\alpha'_P \Delta \ln^2(s/s_0)$.
In the language of Regge poles the multiparticle production processes are related to cut-Reggeon diagrams. Abramovski, Kancheli and Gribov (AGK) proposed rules [11] for calculating the discontinuity of the matrix element that represent the generalisation of the Optical Theorem for the case of multi-Pomeron exchange. The basic results of AGK needed for the following discussion are: a) There is one and only one cut-plane which separates the initial and final states of the scattering. b) Each cut-Pomeron gives an extra factor of (-2) due to the discontinuity of the Pomeron amplitude. c) Each un-cut Pomeron obtains an extra factor of 2 since it can be placed on both sides of the cut-plane.

4 The Model

We propose to describe single- and double- diffraction processes by such diagrams where any number of Pomeron exchanges is taken into account together with each R of the triple-Reggeon and loop diagrams and as well as the screening corrections are considered, as shown in Fig. 2. In this figure the solid line accompanied with a dashed line corresponds to one Reggeon (Pomeron or secondary-Reggeon) exchange together with any number Pomeron exchange. The double-dashed lines stand for eikonal screening.

The theory does not give any prediction on the structure of the vertices for n Pomeron to m Pomeron transitions. The simplest approximation is to assume an eikonal-type structure. In this approximation the general approach of constructing elastic scattering amplitude with account of enhanced diagrams has been proposed in [12]. Assuming π-meson exchange dominance of multi-Pomeron interaction vertices, the authors summed high order enhanced diagrams iterating

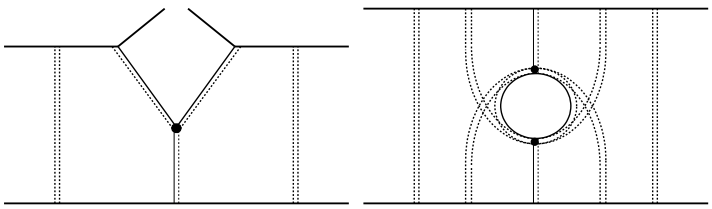

Figure 2: Eikonalised triple-Reggeon and loop diagrams which are proposed to describe single- and double-diffractive processes in hadron-hadron collisions.

multi-Pomeron vertices in both, s- and t- channels. In that article it was demonstrated that the inclusion of these diagrams in most of the cases leads to predictions that are very close to the results of eikonal type models, where a Pomeron with suitably renormalised intercept is used.

For calculating the diagrams shown in Fig. 2 we assume the mentioned π-meson exchange dominance of multi-Pomeron interaction vertex corresponding to the transition of n Pomerons

to m Pomerons:

$$\lambda^{(n,m)} = r_{3P} g_\pi^{n+m-3} \exp\left(-R_\pi^2 \sum_{i=1}^{n+m} q_i^2\right). \tag{3}$$

As a secondary Regge pole we consider f-trajectory. The conservation laws allow us to assume the same pion dominance at the same transition with participation of f-trajectory. In these terms according to the AGK cutting rules, the cross-section corresponding to the cut dressed triple-Reggeon graph for the process $a + b \to X + b$ has the form[1]:

$$\frac{d\sigma}{d\zeta} = \frac{1}{2} \sum_{i,j,k=P,R} G_{ijk} \int d\mathbf{b}\, d\mathbf{b_1}\, \Gamma^i_{b\pi}(\zeta_2, \mathbf{b_2}) \Gamma^j_{b\pi}(\zeta_2, \mathbf{b_2}) \Gamma^k_{a\pi}(\zeta, \mathbf{b_1}) \exp\{-2\Omega_{ab}(\xi, \mathbf{b})\} \tag{4}$$

Here we introduce the following notations

$$\zeta = \ln(M_X^2/s_0),\ \zeta_2 = \xi - \zeta,\ \mathbf{b_2} = \mathbf{b} - \mathbf{b_1},\ \Omega_{\alpha\beta}(\zeta, \mathbf{b}) = \frac{g_{\alpha\beta}}{\lambda_{\alpha\beta}} \exp\left\{\Delta\zeta - \frac{\mathbf{b}^2}{4\lambda_{\alpha\beta}}\right\}, \tag{5}$$

$$\Gamma^P_{\alpha\beta}(\zeta, \mathbf{b}) = 1 - e^{-\Omega_{\alpha\beta}(\zeta, \mathbf{b})},\ \Gamma^R_{\alpha\beta}(\zeta, \mathbf{b}) = \frac{g^R_{\alpha\beta}}{\lambda^R_{\alpha\beta}} \exp\left\{(\alpha_R - 1)\zeta - \frac{\mathbf{b}^2}{4\lambda^R_{\alpha\beta}} - \Omega_{\alpha\beta}(\zeta, \mathbf{b})\right\}.$$

G_{ijk} stand for triple-Regge vertices strength. The expression of the cross-section in the (ζ, t)-space is rather long and we do not present it here.

Analogously can be calculated the cross-section corresponding to the cut dressed loop diagram standing for the process $a + b \to X_1 + X_2$, and it has the following form:

$$\frac{d\sigma}{d\zeta_1 d\zeta_2} = \frac{1}{4} \sum_{i,j,k,l=P,R} G_{ijk} G_{lik} \int d\mathbf{b}\, d\mathbf{b_1}\, d\mathbf{b_2}\, \Gamma^i_{\pi a}(\zeta_1, \mathbf{b_1}) \Gamma^l_{\pi b}(\zeta_2, \mathbf{b_2}) \Gamma^j_{\pi\pi}(\zeta_3, \mathbf{b_3}) \Gamma^k_{\pi\pi}(\zeta_3, \mathbf{b_3})$$
$$\times \exp\{-2\Omega_{ab}(\xi, \mathbf{b}) - 2\Omega_{a\pi}(\xi - \zeta_1, \mathbf{b} - \mathbf{b_1}) - 2\Omega_{b\pi}(\xi - \zeta_2, \mathbf{b} - \mathbf{b_2})\} \tag{6}$$

Here in addition to (5) we used the following notations:

$$\zeta_1 = \ln(M_{X_1}^2/s_0),\ \zeta_2 = \ln(M_{X_2}^2/s_0),\ \zeta_3 = \xi - \zeta_1 - \zeta_2,\ \mathbf{b_3} = \mathbf{b} - \mathbf{b_1} - \mathbf{b_2}$$

5 Extraction of the Parameters from Experimental Data

Because we do not consider the contribution of the enhanced diagrams in the elastic scattering amplitude it allows us to differentiate data fitting procedure and realise it by two steps. At the first step we fix secondary-Reggeon and Pomeron parameters. The trajectories of secondary-Reggeons are fixed from fit to data on spin vs. mass for corresponding family of mesons, and the following results are found: $\alpha_f(t) = 0.7 + 0.8t$, $\alpha_\omega(t) = 0.4 + 0.9t$, $\alpha_\rho(t) = 0.5 + 0.9t$. Then the residues of secondary-Reggeons and the residues/trajectory of Pomeron are found from fit to data on elastic scattering and total interaction cross-section. At the second step we fix triple-Reggeon interaction vertices' constants from fit to data on high mass soft-diffraction dissociation, using the values of the parameters fixed in the first step as an input.

We take into account P-, f- and ω- poles in pp and $p\bar{p}$ elastic scattering amplitude. Since we assume pion exchange dominance at the coupling of Reggeons, we fix the parameters of

[1] If the transferred momentum is very low and the mass of the diffracted system is high the π-meson exchange plays an important role. This we take into account based on the OPER model [13].

secondary Reggeon- and Pomeron- pion coupling as well. In $\pi^{\pm}p$ elastic scattering amplitude, we take into account P-, f- and ρ- poles. Thus, we assume $M = M_P + M_f \pm M_\omega$ for pp and $p\bar{p}$ collisions and $M = M_P + M_f \pm M_\rho$ for π^+p and π^-p collisions, respectively. For Pomeron-trajectory we have found the following parameterisation: $\alpha_P(t) = 1.117 \pm 0.252t$, and other parameters are listed in the Tables 1 and 2.

Table 1: p+$p(\bar{p})$ interaction parameters in GeV^{-2} units.

g_N	$= 1.366 \pm 0.004$
R_N^2	$= 1.428 \pm 0.006$
g_N^f	$= 2.871 \pm 0.008$
R_N^{f2}	$= 0.918 \pm 0.023$
g_N^ω	$= 2.241 \pm 0.074$
$R_N^{\omega 2}$	$= 0.945 \pm 0.026$

Table 2: $\pi^{\pm}p$ interaction parameters in GeV^{-2} units.

g_π	$= 0.85 \pm 0.0004$
R_π^2	$= 0.5 \pm 0.002$
$g_{\pi N}^f$	$= 3.524 \pm 0.001$
$R_{\pi N}^{f2}$	$= 1. \pm 0.001$
$g_{\pi N}^\rho$	$= 1.12 \pm 0.017$
$R_{\pi N}^{\rho 2}$	$= 9.19 \pm 0.837$

Table 3: Found values of G_{ijk} in GeV^{-2} units.

G_{PPP}	$=0.0098 \pm 0.0005$
G_{PPR}	$=0.03 \pm 0.004$
G_{RRP}	$=0.005 \pm 0.001$
G_{RRR}	$=0.05 \pm 0.002$
G_{PRP}	$=0.013 \pm 0.001$
G_{PRR}	$=0.033 \pm 0.005$

Next we fix the triple-Reggeon vertices strengths (G_{ijk}) from fit to data on soft single-diffraction dissociation in pp and $p\bar{p}$ interactions. We used the available data on spectra of non-diffracted proton from fixed-target experiments [14] and [15], from ISR [16] and from CDF [4]. Being interested in soft diffraction, we have chosen measurements done for $d^2\sigma/d\zeta dt$ within the diffractive cone ($-t \leq 0.2\,\mathrm{GeV}^2$). The values of G_{ijk} found are reported in Table 3 and the fit result is compared with data in Figs. 3-5.

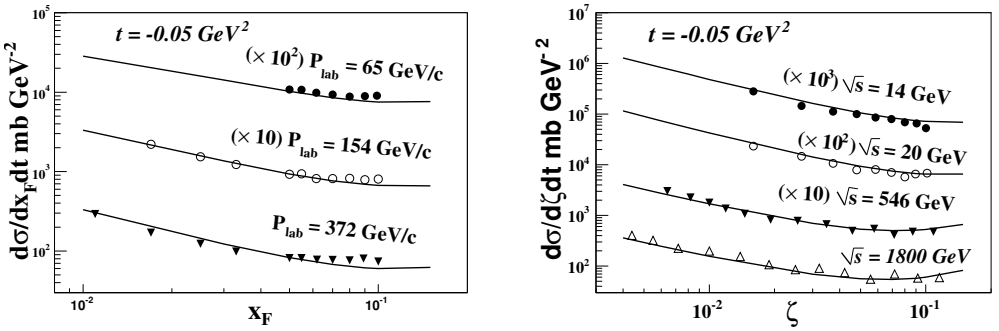

Figure 3: Double differential cross-section $d^2\sigma/d\zeta dt$ for $p(\bar{p}) + p \to p(\bar{p}) + X$ measured at Fermilab at various $\sqrt{s}$ and fixed t. The data are taken from [4, 15].

In Fig. 6 we compare predictions of the model on single-diffractive integrated cross-sections with experimental data [17]. In each case the integration is done in accordance with the corresponding measurement as they are indicated in the figure.

In Fig. 7 we compare predictions of the model on double-diffractive integrated cross-sections with experimental data [18, 19]. The data at $\sqrt{s}$ >100 GeV correspond to the cross-section for minimum 3 units of rapidity gap between two produced clusters and are taken from [18]. The rest of data (at $\sqrt{s}$ <100 GeV) are taken from [19] where exclusively and semi-inclusively measured data are reduced to totally inclusive cross-section. The theoretical curve is calculated using Eq. (6) and requiring minimum 3 units of rapidity gap between two diffracted clusters.

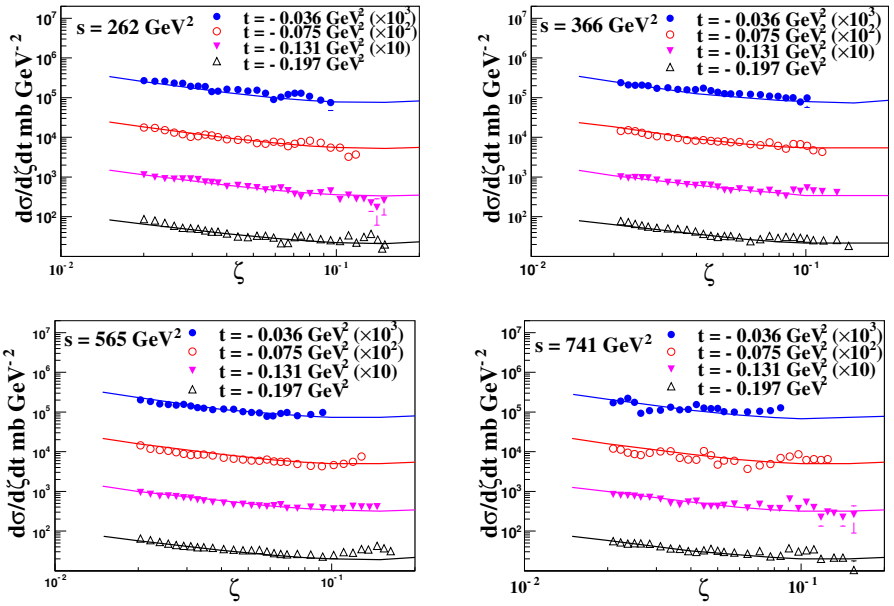

Figure 4: Double differential cross-section $d^2\sigma/d\zeta dt$ for $pp \to pX$ measured at Fermilab at various $\sqrt{s}$ and t. The data are taken from [14].

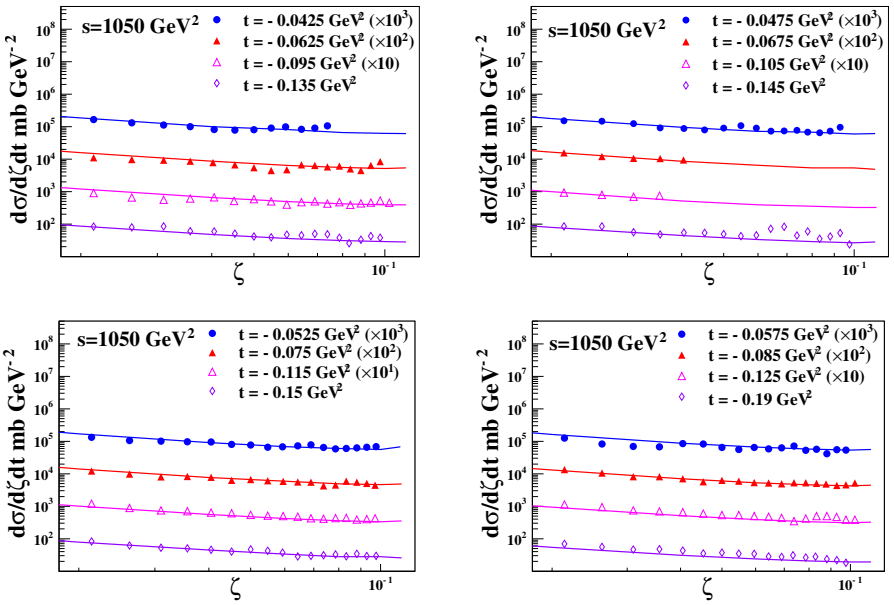

Figure 5: Double differential cross-section $d^2\sigma/d\zeta dt$ for $pp \to pX$ measured at ISR at various $\sqrt{s}$ and t. The data are taken from [16].

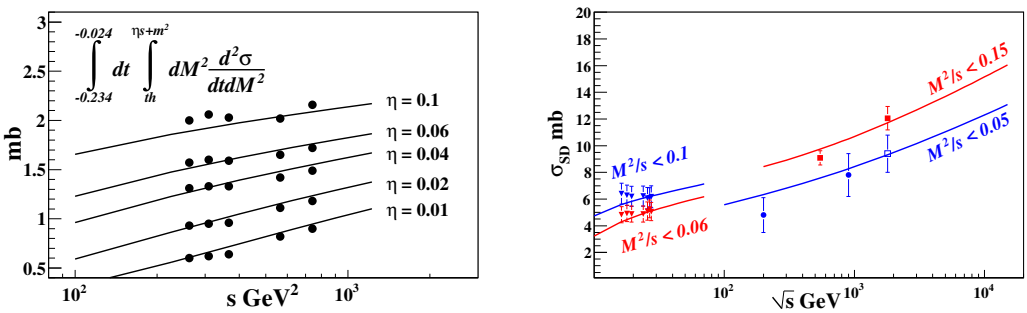

Figure 6: Integrated single-diffractive cross-section as a function of $\sqrt{s}$. The integrations are done in accordance with corresponding measurement as they are indicated in the plots.

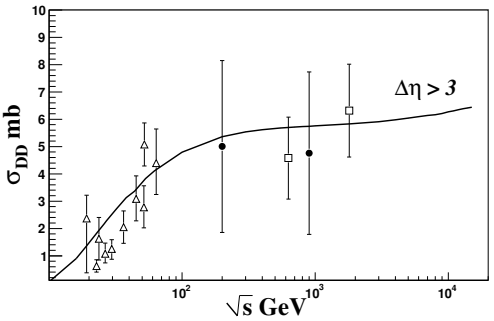

Figure 7: Double-diffractive cross-section as a function of $\sqrt{s}$. The theoretical curve is calculated requiring minimum 3 units of rapidity gap between two diffracted clusters.

6 Summary and Predictions for LHC

In this article we report the results of calculations of all non-enhanced absorptive corrections to triple-Regge vertices and loop diagrams in eikonal approximation using Gribov's Reggeon calculus. Numerically evaluating the model we have found a good description of data on high-mass soft diffraction dissociation in the energy range from ISR, FNAL to Tevatron (from $P_{lab} = 65\,\mathrm{GeV/c}$ to $\sqrt{s} = 1800\,\mathrm{GeV}$). It is worth to emphasise that such a detailed description of inclusive diffraction in this broad region of energies is achieved for the first time. In Table 4 we present the predictions of the model on single- and double- diffractions cross-section for different energies of LHC. The single-diffractive cross-section is obtained integrating over masses up to $M^2/s = 0.05$, and the double-diffractive cross-section is obtained requiring minimum 3 units of rapidity gap between two diffracted clusters.

$\sqrt{s}$ TeV	σ_{SD} mb	σ_{DD} mb
0.9	8.2	5.7
7	11.6	6.1
10	12	6.2
14	13	6.4

Table 4: Predictions for LHC.

Acknowledgements

We thank A. Grigiryan, J.-P. Revol and K. Safarik for their interest in this work.

References

[1] A.B. Kaidalov, Phys. Rep. **50** 157 (1979).

[2] A.B. Kaidalov *et al.*, Phys. Lett. **B45** 493 (1973); JETP Lett. **17** 440 (1973).

[3] A. Donnachie and P.V. Landshoff, arXiv:hep-ph/0305246;
R. Fiore *et al.*, Phys.Rev. **D61** 034004 (2000).

[4] K. Goulianos and J. Montanha, Phys. Rev. **D59** 114017 (1999).

[5] E. Erhan and P. Schlein, Phys. Lett. **B427** 389 (1998).

[6] E. Gotsman *et al.*, Phys. Rev. **D49** R4321 (1994).

[7] E.G.S. Luna *et al.*, Eur. Phys. J. **C59** 1 (2009).

[8] E.S. Martynov and B.V. Struminsky, Yad.Fiz. **59** 1817 (1996) [Physics of Atomic Nuclei **59** 1755 (1996)].

[9] A.B. Kaidalov, Nucl. Phys. **A525** 39c (1991).

[10] K.A. Ter-Martirosyan, Preprints ITEP No. 70, 71 (1975); No. 7, 11, 133, 134, 135, 158 (1976).

[11] V.A. Abramovski, O.V. Kanceli and V.N. Gribov, Sov. J. Nucl. Phys. **18** 308 (1974).

[12] A.B. Kaidalov, L.A. Ponomarev and K.A. Ter-Martirosyan, Sov. J. Nucl. Phys. **44** 483 (1986).

[13] K.G. Boreskov *et al.*, Sov. J. Nucl. Phys. **15** 203 (1972); **17** 669 (1973); **19** 565 (1974).

[14] R.D. Schamberger *et al.*, Phys. Rev. **D17** 1268 (1978).

[15] Y. Akimov *et al.*, Phys. Rev. Lett. **39** 1432 (1977).

[16] J.C.M. Armitage *et al.*, Nucl. Phys. **B194** 365 (1982).

[17] R.E. Ansorge *el al.*, Z. Phys. **C33** 175 (1986); G.J. Alner *et al.*, Phys. Rept. **154** 247 (1987); F. Abe *et al.*, Phys. Rev. **D50** 5535 (1994); N. Amos *et al.*, Phys. Lett. **B301** 313 (1993).

[18] T. Affolder *et al.*, Phys. Rev. Lett. **87** 141802-1 (2001).

[19] G. Alberi and G. Goggi, Phys. Rept. **74** 1 (1981).